# Electron mobility in neon at high densities

A. F. Borghesani, L. Bruschi, M. Santini, and G. Torzo
*Dipartimento di Fisica "Galileo Galilei," Università degli Studi di Padova, I-35131 Padova, Italy*
*and Gruppo Nazionale Struttura della Materia, I-35131 Padova, Italy*
(Received 31 July 1987)

The electron drift mobility has been measured in a wide range of temperatures and densities in neon gas and saturated vapor. The "zero-field" density-normalized mobility $\mu_0 N$ exhibits a strong density dependence, which cannot be accounted for by the existing multiple-scattering theories. The data, however, can be well fitted by assuming a density dependence in the $e$-Ne scattering cross section.

## I. INTRODUCTION

### A. Electron mobility at low density

The classical prediction for the mobility $\mu$ is given by the well-known relation[1]

$$(\mu N)_0 = -\frac{e}{3}\left[\frac{2}{m}\right]^{1/2}\int_0^\infty \frac{\varepsilon}{\sigma_M(\varepsilon)}\frac{dg(\varepsilon)}{d\varepsilon}d\varepsilon\ , \tag{1}$$

where $m$ and $e$ are the mass and the electric charge of the electron, $\sigma_M(\varepsilon)$ is the momentum-transfer cross section at the energy $\varepsilon$, and $N$ is the number density of the scattering gas. The function $g(\varepsilon)$ is given by

$$g(\varepsilon)=D\exp\left[-\int_0^\varepsilon\left[\frac{M(E/N)^2e^2}{6m\varepsilon'\sigma_M^2(\varepsilon')}+k_BT\right]^{-1}d\varepsilon'\right]\ , \tag{2}$$

where $M$ is the atomic mass of the gas, $E$ the electric field, $k_B$ the Boltzmann constant, and $T$ the absolute temperature. The constant $D$ is fixed by the normalization of the energy distribution function $f(\varepsilon)=\sqrt{\varepsilon}g(\varepsilon)$. This classical result is valid when multiple and inelastic collisions can be neglected. At very low values of $E/N$, $f(\varepsilon)$ becomes

$$f(\varepsilon)=D\sqrt{\varepsilon}\exp(-\varepsilon/k_BT)\ , \tag{3}$$

with $D=2/[\pi(k_BT)^3]^{1/2}$. In this case

$$(\mu_0 N)_0=\frac{4e}{3(2\pi mk_BT)^{1/2}\sigma^*}=\frac{B(T)}{\sigma^*}\ , \tag{4}$$

where $B(T)=4e/3(2\pi mk_BT)^{1/2}$ and $\sigma^*$ has the dimension of a scattering cross section defined by

$$(\sigma^*)^{-1}=(k_BT)^{-2}\int_0^\infty\frac{\varepsilon\exp(-\varepsilon/k_BT)}{\sigma_M(\varepsilon)}d\varepsilon\ . \tag{5}$$

The density-normalized "zero-field" mobility $(\mu_0 N)_0$ is independent of $E$ and $N$.

In the general case $(\mu N)_0$ must be numerically calculated through Eqs. (1) and (2). As an example we show in Fig. 1 the result obtained for neon at the liquid nitrogen temperature, using the $\sigma_M(\varepsilon)$ proposed by O'Malley and Crompton[2] (Fig. 2). As $\sigma_M$ is very small, the field-independent region is reached only at very low values of the reduced field $E/N$.

### B. Electron mobility at high density

At high densities, where the mean free path $l$ becomes comparable with the electron thermal wavelength $\lambda$, multiple scattering effects must be taken into account. As a result, $\mu_0 N$ at low fields is no longer density independent as in the classical case. If we plot $\mu N$ as a function of $E/N$ for different densities we get different curves, which meet the unique classical dependence only at high values of the reduced field (see Fig. 1).

For rare gases with a negative scattering length $a$ (argon, krypton, xenon), it has been found a "positive" effect, i.e., $\mu_0 N$ increases with $N$. In helium and hydrogen, for which $a$ is positive, the density effect is "negative," i.e., $\mu_0 N$ decreases with $N$.[3]

Theories which take multiple scattering into account have been developed in the limit of $(E/N)\to 0$. They assume that the electron-atom cross section is only weakly dependent on the energy $\varepsilon$. For the negative effect and

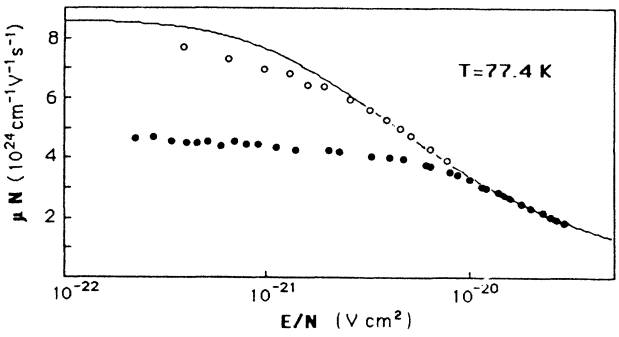


FIG. 1. Some experimental data of density-normalized mobility $\mu N$ vs the reduced electric field $E/N$ in neon at 77.4 K. Open dots: $N=7.7\times10^{20}$ cm$^{-3}$. Closed dots: $N=44.3\times10^{20}$ m$^{-3}$. Solid curve: classical prediction [Eq. (1)].

 

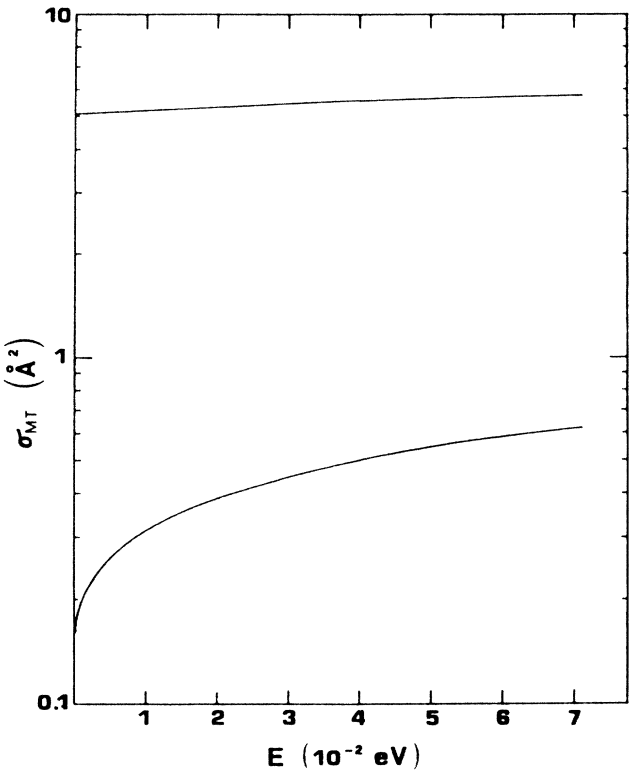


FIG. 2. Momentum-transfer cross section $\sigma_M$ vs electron energy $\varepsilon$ for helium (upper curve) and for neon (lower curve) (Ref. 2).

not too high density, the results of O'Malley[4] and of Braglia and Dallacasa[5] can be summarized as

$$\mu_0 N = (\mu_0 N)_0 \exp\left[-\frac{\lambda \sigma_T N}{\sqrt{\pi}}\right], \tag{6}$$

where $\mu_0 N$ is the "zero-field" density-normalized mobility, $(\mu_0 N)_0$ is its corresponding classical low-density expression, $\sigma_T$ is the total electron-atom scattering cross section, and $\lambda = h/\sqrt{2\pi m k_B T}$ is the thermal electron wavelength.

For low densities Eq. (6) can be approximated as

$$\mu_0 N = (\mu_0 N)_0 \left[1 - \frac{\lambda \sigma_T}{\sqrt{\pi}} N\right]. \tag{7}$$

The same linear dependence, but with 0.5 in place of $1/\sqrt{\pi}$, has been proposed by Atrazhev and Iakubov,[6] and by Schwarz.[7] The scattering cross sections $\sigma_T(\varepsilon)$ and $\sigma_M(\varepsilon)$ are assumed to depend very weakly on $\varepsilon$ at thermal energies, so that they are approximated by constant values $\sigma_T$ and $\sigma_M$. By using Eq. (4) with $\sigma^* = \sigma_M$, and the expression for $\lambda$, we can write Eq. (7) as follows:

$$\mu_0 N = (\mu_0 N)_0 - \alpha N, \tag{8}$$

where

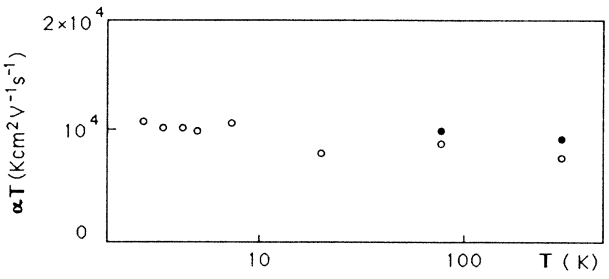


FIG. 3. Product $\alpha T$ vs temperature $T$ in helium (open dots) and in $H_2$ (closed dots) from Refs. 7 and 17.

$$\alpha = \frac{2eh}{3(\pi)^{3/2} m k_B T} \frac{\sigma_T}{\sigma_M}. \tag{9}$$

Because at thermal energies $\sigma_T/\sigma_M \approx 1$, the slope of the linear plot is independent of the particular gas, and the product $\alpha T = 1.01 \times 10^4$ K cm$^2$/V s is a temperature-independent constant, the same for all gases with a positive scattering length. This prediction is rather well satisfied by the experimental results obtained in He and $H_2$ in a wide temperature range (Fig. 3).

Among the rare gases neon is situated in between the opposite behavior of gases with positive and negative scattering lengths. As a result of the good balance between the attractive and repulsive part of the electron atom interaction, it shows a small, but positive, scattering length ($a \approx 0.1$ Å to be compared with $a \approx 0.63$ Å for He). The effect should be negative, as for He and $H_2$. But according to (6) the relative change in $\mu_0 N$ must be weaker, owing to the smallness of $\sigma_T$. In this sense, therefore, we should expect a negative and weak multiple-scattering correction to the classical mobility.

In a first set of measurements with the square-wave method,[8] we found indeed a negative effect. However, it was much stronger than expected and the prediction $\alpha T = \text{const}$ was not followed.[9,10] To test these results we repeated the measurements with the photoelectric method (Sec. II B). This second set of results is the main subject of the present paper.

## II. EXPERIMENTAL

### A. Cryogenics and gas handling

The measuring cell was cooled by a model 21 CTI Cryocooler. The temperature was measured by a calibrated Pt resistance (Rosemount 118MF 500), and stabilized in the range 25–300 K to within ±0.05 K.[11,12] The gas pressure was measured by an Ashcroft Digigauge model 7780, and the neon gas density was calculated by means of the McCarty-Stewart equation.[13] In "pure" gases, as those supplied for research purposes,[14] diatomic molecular species such as $N_2$ and $O_2$ are always present as impurities (concentration $C \approx 1$ ppm). Such species are also released by the surfaces of the gas handling plant and by the measuring cell itself. These impurities are very effective in thermalizing hot electrons by means of inelas-

tic collisions (see Sec. III). Moreover, in the case of oxygen a fraction of the inelastic collisions produces stable and very slow negative ions. The efficiency of this process increases rapidly at high densities.[15] It removes electrons from the fast swarm, creating an ionic space-charge electric field that may become comparable with the applied electric field, especially at low fields.[8–10] For these reasons the impurity content must be kept as low as possible.

We used an Oxisorb[16] trap to remove oxygen and a cold activated-charcoal trap to remove both $N_2$ and $O_2$. To increase the trap efficiency the high-pressure gas is forced to circulate many times in a closed loop including both traps and the measuring cell. We developed a circulator free from moving parts to be sealed. A stainless-steel thin-walled bellow is slowly compressed and released, displacing a gas volume of 4 $cm^3$ each cycle. The inner volume of the bellow is connected to the gas loop through inlet-outlet spring valves. The bellow is immersed in a degassed oil bath, which is driven by a high-pressure oil displacer. The oil pressure adjusts itself to the gas pressure by a very small bellow expansion and therefore the thin-walled bellow can safely work in high-pressure conditions.

### B. The pulsed photoemission method (PPM)

The pulsed photoemission method is a well known and widely used method.[17] A constant potential difference $V$ is applied between two circular, plane, parallel electrodes of radius $r$, separated by a gap $d$ (Fig. 4). A thin slice of $n$ electrons is extracted from the cathode by means of a narrow uv radiation pulse. The electrons drift at velocity $v_d$ under the influence of the electric field $E=V/d$, and a current $i$ sets in the circuit. If $d \ll r$, $i=-env_d/d$. If electrons drift in a gas with negligible attachment, $v_d$ and $n$ are constant. In this case $i=$const for $0<t<\tau=d/v_d$. From the analysis of the current waveform we easily get the drift velocity $v_d$.

The most important feature of this method is the absence of negative-ion pileup. In fact, if the time between successive pulses is made greater than the ionic transit time, we are dealing only with impurity ions produced by a single pulse, a much better working condition with respect to the square-wave method previously used.[8]

In Fig. 4 we show a schematic of the measuring apparatus. The uv radiation enters the cell through a first thick "seal" fused silica window, and it impinges on a thin metal film (Au, 100 Å) evaporated onto the inner surface of a thinner-fused silica window. The film acts as the active area of the emitter electrode. The seal window must withstand both gas pressures up to 10 MPa and large stresses arising from the difference between the thermal expansion coefficients of fused silica and common metal. We solved this problem by gluing the thick window with epoxy resin to a compensating Invar collar, previously soldered onto the top flange. Details on the photocathode and on the seal window are described elsewhere.[18]

The signal preamplifier has a gain of 100 and it is placed close to the cell in order to minimize the parasitic

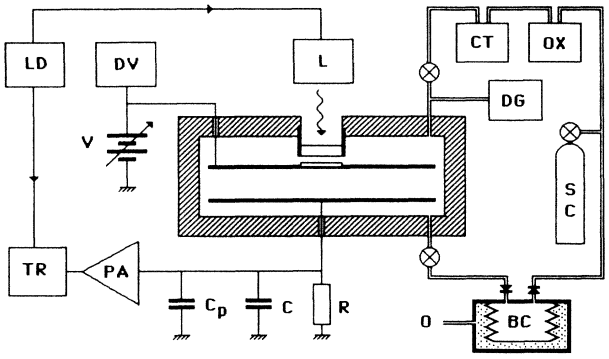


FIG. 4. Schematic diagram of the experimental apparatus. L: flash lamp; LD: lamp diver; PA: preamplifier; TR: transient recorder; DV: digital voltmeter; V: regulated power supply; CT: cold trap; OX: Oxisorb; BC: bellow circulator; DG: Ashcroft Digigauge; O: oil displacer. $R=1\times10^9\ \Omega$, $C=10$ pF, $C_p=30$ pF.

capacitance $C_p$. For a faithful reproduction of the current waveform of duration $\tau$ we must choose $RC_T \ll \tau$, where $C_T=C_P+C$. Because $C_P \approx 30$ pF, the maximum allowed input resistance $R$ would yield a small voltage signal $V^-(t)=Ri(t)$. It is therefore more convenient to use a high-load resistance ($RC_T \gg \tau$) looking at the integrated signal waveform. With a very short flash lamp pulse ($\Delta T \ll \tau$), and for constant current $i_0=-en/\tau$, we get

$$V^-(t)=\begin{cases} 0 \quad \text{for } t<0 & \text{(10a)} \\ \dfrac{-en}{C_T}\dfrac{t}{\tau} \quad \text{for } 0\le t\le\tau & \text{(10b)} \\ V_0^-=-en/C_T \quad \text{for } t>\tau\ . & \text{(10c)} \end{cases}$$

The time of flight is easily measured from the integrated waveform, as shown in Fig. 5.

When oxygen impurities are present, $i(t)=i_0\exp(-\nu_A t)$, where $\nu_A$ is the attachment frequency. The integrated waveform is given by

$$V^-(t)=\begin{cases} \dfrac{V_0^-}{\tau\nu_A}[1-\exp(-\nu_A t)] \quad \text{for } 0\le t\le\tau & \text{(11a)} \\ V^-(\tau)=V_{\max}^- \quad \text{for } t\ge\tau\ . & \text{(11b)} \end{cases}$$

When the signal waveform differs from a straight line, it means that the impurity concentration is relevant. By circulating the gas through the traps the waveform becomes less and less bended, approaching the linear behavior predicted by (10), while $V_{\max}^-$ increases progressively towards $V_0^-$. Monitoring the signal shape, therefore, allows us to evaluate the degree of purity of the gas.

Our uv pulses are generated by a commercial flash lamp (EG&G, model FX108AU) and they have a width

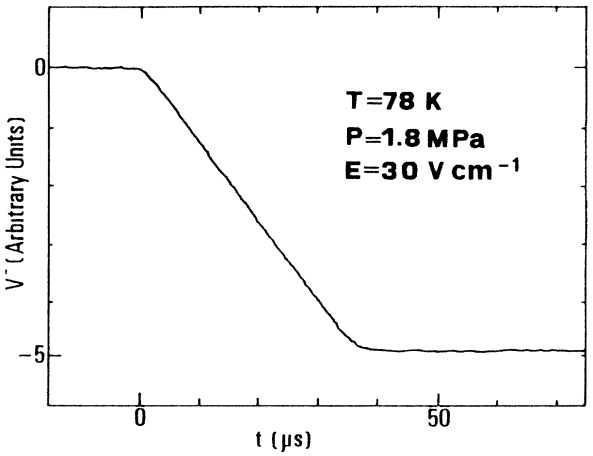


FIG. 5. Record of the integral collector signal at a temperature $T=48$ K, a pressure $P=1.8$ MPa, and with an applied electric field $E=30$ V/cm.

$\Delta t \approx 4$ μs. In most experimental situations $\Delta t$ is not negligible with respect to $\tau$. The starting and final parts of the signal are rounded off for a time $\tau^* \approx \Delta t$, as not all the $n$ electrons have yet entered (or left) the drift space. When all the electrons are present in the drift space, however, the current is constant, and $V^-$ increases linearly with time: $V^- = (V_0^-/\tau)t + V^{-'}$. The extrapolation of this line (Fig. 5) crosses the $t$ axis at $t' = -\tau V^{-'}/V_0^-$, and the plateau ($V^- = V_0^-$) at $t'' = \tau(1 - V^{-'}/V_0^-)$. The time of flight is given by $\tau = t'' - t'$.

It is usually difficult to fulfill the condition $r \gg d$ in a practical experiment. For small $d$, $\tau$ is small and it cannot be measured with good accuracy especially with rather wide uv pulses. On the other hand, a large measuring cell must be very massive to withstand high pressures. In an actual experiment $r$ and $d$ will be of the same order, $r \approx d$. In this situation the signal waveform is far from being linear, even for negligible attachment ($\nu_A \approx 0$). It is therefore difficult to estimate whether a possible attachment has distorted such a waveform from its ideal shape. For this reason it is convenient to choose a ratio $r/d$ for which the signal waveform at $\nu_A \approx 0$ is linear to a reasonable accuracy. A detailed calculation shows that $r/d \approx 2$ represents an acceptable compromise. In our final high-pressure cell we chose $d=1$ cm and $r=3$ cm. More details on the intricate problem of the signal waveform can be found in another paper, where we report results of the numerical calculations, and experimental checks performed with various cell geometries.[19]

## III. EXPERIMENTAL RESULTS

After a long outgassing at room temperature and several flushes with pure gas, neon was compressed in the gas loop,[8] with the measuring cell at the selected temperature. The waveform was periodically tested at low fields while circulating the gas, as explained in Sec. II A. When the shape was linear and the amplitude was saturated to its maximum, the circulation was stopped. The drift velocity $v_d$ was measured, at fixed $T$ and $N$, as a function of the applied field $E$.

Even the check of signal linearity and amplitude saturation, however, may be not sufficient to assure that the gas is appropriately purified. In Fig. 6 we report, as an example, a result obtained at $T=293$ K and $N = 1.9 \times 10^{20}$ cm$^{-3}$, as previously described. The values of $v_d$ at high $E/N$ are larger than predicted by the classical theory. In the log-log plot almost all the data lie on a straight line, as if the electrons were thermalized also at high fields. A possible explanation is that this thermalization is reached through inelastic collisions with residual diatomic impurities ($O_2$,$N_2$). In fact, circulating the gas for some more hours, the data at high fields dropped progressively onto the classical curve. After the circulator was stopped, the measured $v_d$ increased slowly with time, as if impurities were slowly released by the cell walls. This effect is much more sensitive to the impurities content than the waveform shape, and it shows that for gases with small cross section the measurements at high densities are rather delicate. The data reported in this paper were taken after a circulation of several hours.

After the previously described checks, the mobility $\mu = v_d/E$ was measured, at fixed $T$ and $N$, as function of $E$ down to the smallest electric fields. The results at high fields turned out to be in agreement with the classical dependence calculated with the gas-phase scattering cross section[2] (Fig. 1). The mobility data at low fields are lower than the classical ones. Their extrapolation at $E=0$ yields the so called zero-field mobility $\mu_0$. If the density is not too low, this extrapolation can be made with reasonable confidence. At very low densities, however, $\mu$ depends strongly on $E$ even for fields $E \approx 1$ V/cm, and the extrapolation is meaningless. The densities involved in this experiment were normally greater then $2.0 \times 10^{20}$ cm$^{-3}$.

The results obtained at $T=293$, 196, and 47.9 K are shown in Figs. 7–9, respectively, as $\mu_0 N$ versus $N$. These and other similar data can be extrapolated at $N=0$ to get the density-normalized mobility $(\mu_0 N)_0$. Its values slightly depend on the extrapolation procedure. As an example, we list in Table I the values obtained by fitting the data with a second-order polynomial, and with an ex-

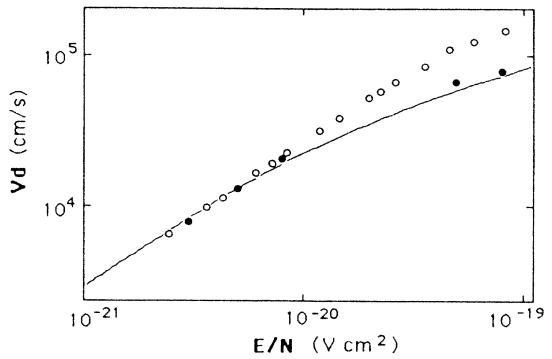


FIG. 6. Electron drift velocity $v_d$ vs the reduced field $E/N$ at $T=293$ K and $N = 1.9 \times 10^{20}$ cm$^{-3}$. Open dots: preliminary purification. Closed dots: after circulation through the purifiers for some hours.

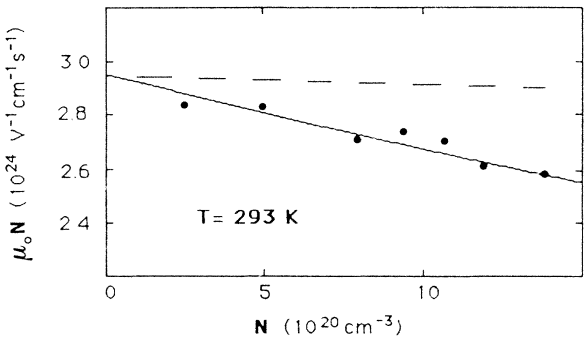


FIG. 7. Measured $\mu_0 N$ vs gas density $N$ at $T=293$ K. Dashed line: Eq. (6). Solid line: Eq. (19).

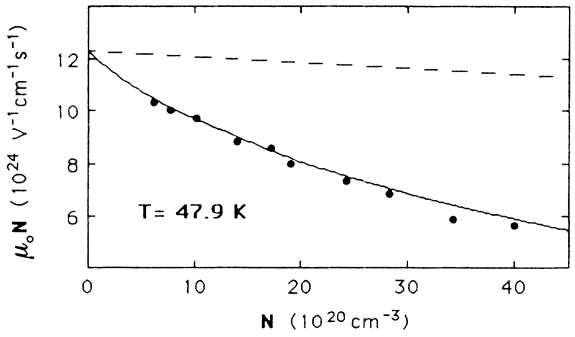


FIG. 9. Measured $\mu_0 N$ vs gas density $N$ at $T=47.9$ K. Dashed line: Eq. (6). Solid lines: Eq. (19).

ponential function, as suggested by Eq. (6). In any case there is a good agreement with the values calculated by means of Eqs. (4) and (5) using the scattering cross section of O'Malley and Crompton.[2]

The density dependence is stronger than predicted by Eq. (6), in agreement with our previous result. There are slight differences in the density dependence between the two sets of data, which may be due to systematic errors introduced by our previous technique or to different degrees of purification.

In Fig. 10 we report the results obtained in saturated vapor between 25.7 and 40.6 K. In this case we have only one density at each temperature, and so the data are simply plotted as a function of the temperature $T$.

## IV. DISCUSSION

### A. Qualitative considerations

In the absence of a general theory we try to explain our experimental results on the basis of the following qualitative discussion. We know that multiple scattering effects, as accounted for by Eq. (6), describe well the density dependence of $\mu_0 N$ in He and $H_2$. These effects, therefore, must be certainly present also in high-density neon. But here $\sigma_T$ is smaller, and Eq. (6) predicts only a minor correction to the classical theory (see Figs. 7–10).

The present data, on the other hand, confirm the main point reached in our previous experiment. The density dependence of $(\mu_0 N)$ in Ne is stronger than predicted by the existing multiple scattering theories. This dependence increases as the temperature is lowered. We should therefore look for a different density effect, which becomes stronger at lower temperatures, and which is negligible for He and $H_2$.

The most relevant difference between He and Ne is the behavior of the scattering cross sections at low energies (Fig. 2). For instance, while $\sigma_M(\varepsilon)$ is about 5 Å$^2$ in He and it changes by only 11% from $\varepsilon=0$ to $\varepsilon=4\times10^{-2}$ eV, in Ne it is ten times smaller, and in the same energy range it changes by a factor of 3, that is, from 0.16 Å$^2$ to 0.49 Å$^2$. The different behavior of the density-normalized mobility $\mu_0 N$ for these two systems must therefore be connected to the different behavior of the scattering cross section, and one has to look for a physical effect that may induce a density dependence on the effective scattering cross section.

The magnitude and the energy dependence of the scattering cross section in Ne is the result of a good balance between the attractive and repulsive contribution to the electron-atom interaction. At very high densities, the effective scattering potential can differ from that in the dilute phase, as a result of the overlap of the polarization tails, and the effective scattering cross section may be density dependent. This effect has been considered in the well-studied case of liquid argon,[20,21] and the inadequacy of the gas-phase scattering cross section has been pointed out also for liquid and solid Ne.[22] Our densities, howev-

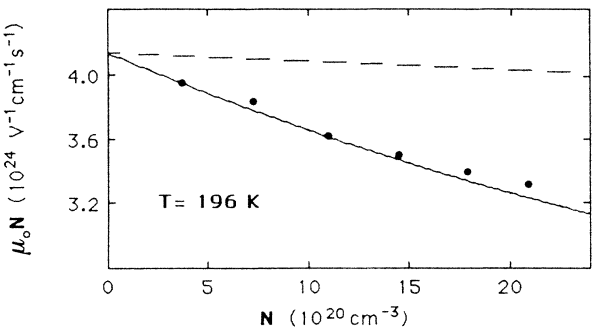


FIG. 8. Measured $\mu_0 N$ vs gas density $N$ at $T=196$ K. Dashed line: Eq. (6). Solid line: Eq. (19).

TABLE I. The zero-field density-normalized mobility $\mu_0 N$ is expressed in $(10^{24}\ \mathrm{V\,cm\,s})^{-1}$. Column labeled 1: zero-density values extrapolated by using an exponential function. Column labeled 2: zero-density values extrapolated by using a second-order polynomial. Column labeled 3: classical prediction equations (4) and (5).

| $T$ (K) | 1 $(\mu_0 N)_0$ | 2 $(\mu_0 N)_0$ | 3 $(\mu_0 N)_{\mathrm{Cl}}$ |
|---|---|---|---|
| 293 | 2.93 | 2.87 | 2.95 |
| 196 | 4.10 | 4.16 | 4.14 |
| 101 | 6.77 | 6.86 | 7.02 |
| 77.4 | 8.55 | 8.84 | 8.63 |
| 47.9 | 11.60 | 11.66 | 12.35 |

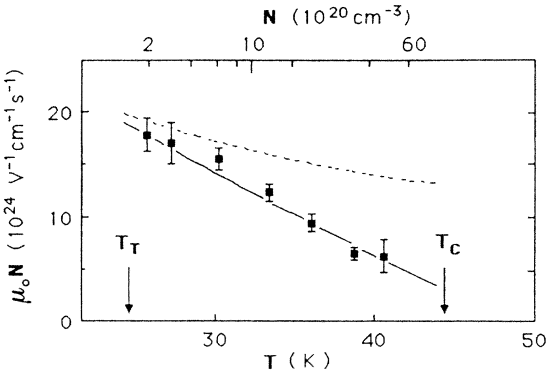


FIG. 10. Measured $\mu_0 N$ vs temperature $T$, in saturated vapor. $T_T$: triple-point temperature. $T_c$: critical-point temperature. Dashed line: Eq. (6). Solid lines: Eq. (19).

er, are not so high for this effect to be relevant. We have found in fact that at large $E/N$ the data are in quite good agreement with those calculated with the gas-phase scattering cross section even at the highest densities used in our experiment.

The result of multiple scattering expressed by Eq. (6) has been obtained for a constant scattering cross section, and therefore neglects a second possible multiple-scattering effect due both to the energy dependence of the scattering cross section and to the Fermi shift.[23] For helium this second effect would be weak with respect to the first one, owing to the weak energy dependence of the $\sigma_M$. The opposite situation would occur for neon, where $\sigma_T$ is small and $\sigma_M$ depends strongly on the energy. We may take advantage of this fact, accounting for the larger effect in a first step, while introducing the smaller one in a subsequent correction.

### B. Ground state and scattering

To begin with, we look for a modification of the classical result for $(\mu_0 N)_0$, Eqs. (4) and (5), appearing as a first factor in the right-hand side of Eq. (6). It can be suitably written as

$$(\mu_0 N)_0 = \frac{B(T)}{(k_B T)^2}\sqrt{m/2} \times \int_0^\infty \frac{\sqrt{2\varepsilon/m}\,[\sqrt{\varepsilon}\exp(-\varepsilon/k_B T)]}{\sigma_M(\varepsilon)} d\varepsilon \,. \quad (12)$$

The factor inside the square brackets belongs to the energy distribution function, while $\sqrt{2\varepsilon/m}$ is the electron velocity.

The relation (12) is valid only when the density $N$ of the scattering centers is very low. A rigorous treatment of the problem at high densities has not yet been attained. For the present discussion we may refer to a simplified model developed for monoatomic fluids by Springett, Jortner, and Cohen (SJC).[24] They used an average lattice representation together with a pseudopotential model. The electron-atom potential is taken as a sum of a mean, density dependent, negative polarization potential $U_P(N)$, plus a hard-core repulsive Hartree-Fock pseudopotential of the form $V_R = \infty$ for $r < \tilde{a}$, $V_R = 0$ for $r > \tilde{a}$, where $\tilde{a}$ is the positive Hartree-Fock scattering length. Taking into account the result for conduction electrons in metals,[25] the energy of "quasifree" electrons takes the form

$$E = E_0 + \hbar^2 k^2/2m \,, \quad (13)$$

where $k$ is the wave vector, $E_0$ is the density dependent ground state energy, and $m$ is practically the electron mass.

At low densities, $E_0$ can be approximated by the Fermi shift $E_0 \approx (2\pi/m)\hbar^2 aN$, where $m$ is the electron mass, and $a$ is the electron-atom, gas-phase, scattering length.[23] Therefore it can be positive as well as negative, depending on the sign of the scattering length. At higher densities $E_0$ takes the form

$$E_0 = T_0 + U_P \,, \quad (14)$$

where $T_0$ is the zero point kinetic energy which essentially arises from excluding the electron from the hard-core volume. It is calculated with the Wigner-Seitz method. Because the polarization potential $U_P$ is negative, $E_0$ can be positive or negative depending on the relative magnitude of $T_0$ and $U_p$. In helium, as an example, $U_P \ll T_0$, and $E_0$ is essentially kinetic energy.

Owing to local density fluctuations, $E_0$ is not sharply defined, and these fluctuations should be taken into account when computing the density of states.[15,26] To simplify the discussion, however, we neglect the density fluctuations. With this approximation the density of states is given by $g(E)=0$ for $E < E_0$, and $g(E) = A\sqrt{E - E_0}$ for $E \geq E_0$. The energy distribution function is $f(E)=0$ for $E < E_0$, and $f(E) = C\sqrt{E - E_0}\,e^{-E/k_B T}$ for $E \geq E_0$. Imposing the normalization condition we get $C = D\exp(E_0/k_B T)$, where $E$ is the constant defined in Eq. (3). The classical distribution (3) is then changed into the shifted distribution

$$f(E) = D\sqrt{E - E_0}\exp[-(E - E_0)/k_B T] \quad (15)$$

for $E \geq E_0$, and $f(E)=0$ for $E < E_0$. In this new situation the square brackets in Eq. (12) should be replaced by the analogous expression $\sqrt{E - E_0}\exp[-(E - E_0)/k_B T]$, and the velocity $\sqrt{2\varepsilon/m}$ by the group velocity which, from the dispersion relation (13), is $v_g = \sqrt{2(E - E_0)/m}$. Equation (12) is changed to

$$(\mu_0 N)^* = \frac{B(T)}{(k_B T)^2} \times \int_{E_0}^\infty \frac{(E - E_0)\exp[-(E - E_0)/k_B T]}{\sigma_M(E^*)} dE \,, \quad (16)$$

where $(\mu_0 N)_0$ has been changed to $(\mu_0 N)^*$ to indicate that we are working at moderately high densities. With the substitution $E - E_0 = \varepsilon$ we get

$$(\mu_0 N)^* = \frac{B(T)}{(k_B T)^2} \int_0^\infty \frac{\varepsilon \exp(-\varepsilon/k_B T) d\varepsilon}{\sigma_M(\varepsilon^*)} , \quad (17)$$

that is, simply the classical result $(\mu_0 N)_0$ only if $\sigma_M = \text{const}$. On the other hand, if $\sigma_M$ is strongly energy dependent, it becomes important to define the energy $\varepsilon^*$ at which $\sigma_M$ is calculated. The choice $\varepsilon^* = \varepsilon$ does not bring anything new, since in this case $(\mu_0 N)^* = (\mu_0 N)_0$.

A suggestion for the right choice comes out from the results of the experiments on the resonant attachment of electrons to oxygen molecules, that are present as impurities in the host gas. The attachment is a two-stage process. In the first stage the colliding electron has a defined probability to be captured by a target $O_2$ molecule in its ground state, to form an unstable negative ion $O_2^{-*}$ in the $n=4$ vibrationally excited state. In the second stage the excited ion is eventually stabilized into the ground state.[27] The first one is a resonant process, and the capture cross section $\sigma_c$ depends strongly on the energy, being sharply peaked at the resonant energy $E_R = 0.091$ eV, with a width $\Delta E \approx 2 \times 10^{-4}$ eV. The mean life $\tau_A$ of the drifting electrons is essentially regulated by the probability that they have the correct energy $E \approx E_R$. The value of the so-called attachment frequency $\nu_A = (1/\tau_A)$ can therefore be varied by changing the value of the energy distribution function at $E = E_R$. This is usually accomplished by changing the temperature $T$, or the reduced electric field $E/N$.[27]

It has been discovered, working in high-density helium gas, that $\nu_A$ can be varied by a simple change of the gas density $N$. The attachment frequency $\nu_A$ as a function of $N$ shows, in fact, a pronounced peak, with the maximum at a density $N^* \approx 30 \times 10^{20}$ cm$^{-3}$, for which $(2\pi/m)\hbar^2 \alpha N^* \approx E_R$.[15,28] This experiment has been performed at several temperatures from 45 to 100 K, where the average thermal energy $k_B T$ is small with respect to $E_R$ ($0.04 E_R$ up to $0.1 E_R$). This result therefore suggests that it is the total kinetic energy $(\varepsilon + T_0)$ which enters the capture scattering process, and not the much smaller thermal contribution $\varepsilon$.

### C. Fitting the data

If one puts together the mobility results of the present experiment with those of the resonant attachment in He, it seems reasonable to assume that the momentum-transfer cross section $\sigma_M(\varepsilon)$ appearing in Eq. (17) should be calculated at the energy $\varepsilon^* = \varepsilon + \varepsilon_0$, where $\varepsilon_0$ should be given by the kinetic part $T_0$ of the quantum shift $E_0$. For helium gas it is a very good approximation to use a constant scattering length $a = 0.63$ Å, and to calculate $\varepsilon_0$ with the Wigner-Seitz (WS) model, as shown by the beautiful injection experiment of Broomall *et al.*[29] This approximation is certainly not valid for neon and other atoms which show a strong energy dependence of the scattering cross section.

We have not at present a general theory for a detailed calculation of $\varepsilon_0$, and it is therefore convenient to use again some guess coming out from the experiments. Using Eq. (17) and the gas phase $\sigma_M(\varepsilon + \varepsilon_0)$, we found out the values of $\varepsilon_0$ for which Eq. (17) reproduces the interpolated values of the experimental data. We found that, to within the experimental errors, $\varepsilon_0$ does not depend on the temperature $T$, but it is a function of the density alone. Moreover, it is very close to the function $\varepsilon_0$ one obtains with the WS method using an energy-dependent scattering length. Our results were therefore fitted as follows.

We calculated $\varepsilon_0$ with the Wigner-Seitz model. If $r_s = [3/(4\pi N)]^{1/3}$, the wave vector $k_0 = \sqrt{2m\varepsilon_0}/\hbar$ is given by the well-known WS condition

$$\tan[k_0(r_s - a)] - k_0 r_s = 0 . \quad (18)$$

The radius of the hard-core scatterers is written as $a = (\sigma_T/4\pi)^{1/2}$. The total scattering cross section is calculated at the energy $\varepsilon_0 = (\hbar^2 k_0^2/2m)$.

In other words, the energy shift $\varepsilon_0$ must be computed using a "self-consistent" effective radius $a = \sqrt{\sigma_T(\varepsilon_0)/4\pi}$, where the total scattering cross section $\sigma_T$ is evaluated at the energy $\varepsilon_0$. The result of this calculation performed with the gas phase $\sigma_T$ of O'Malley and Crompton is shown in Fig. 11 as a function of the density $N$. We used $\varepsilon_0(N)$ values calculated in this way to compute $(\mu_0 N)^*$ at several densities through Eq. (17), letting $\sigma_M(\varepsilon^*) = \sigma_M(\varepsilon + \varepsilon_0)$, and using the gas-phase scattering cross section given by O'Malley and Crompton.

The second (and weaker) multiple-scattering effect is then accounted for by using Eq. (6), with $(\mu_0 N)^*$ in place of $(\mu_0 N)_0$. Because it is a weak effect, we may use the approximated form given by expressions (8) and (9), assuming $\sigma_T/\sigma_M = 1$. We finally have

$$\mu_0 N = \frac{3.27 \times 10^{17}}{T^{5/2}} \int_0^\infty \frac{\varepsilon \exp(-1.16 \times 10^4 \varepsilon/T)}{\sigma_M(\varepsilon + \varepsilon_0)} d\varepsilon - \frac{1.01 \times 10^4 N}{T} , \quad (19)$$

where $\mu_0$ is given in cm$^2$/V s, $N$ in cm$^{-3}$, $\sigma_M$ in cm$^2$, and $\varepsilon$ in eV. The results of $\mu_0 N$ calculated through (19) are shown in Figs. 7–9 versus $N$ at constant temperature, and in Fig. 10 versus $T$. The agreement with the experimental data is surprisingly good at all temperatures.

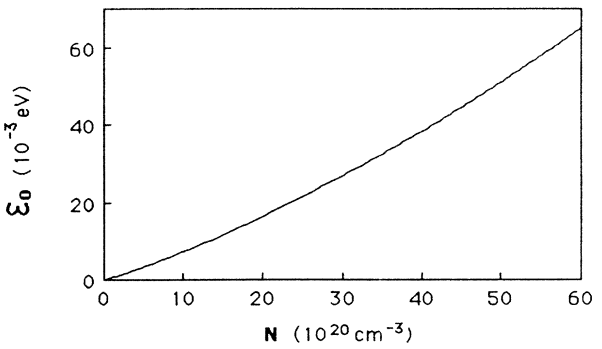


FIG. 11. "Self-consistent" Wigner-Seitz energy $\varepsilon_0$ calculated as explained in the text.

## V. CONCLUSIONS

The results obtained in our previous work with a different method of measurement are essentially confirmed by the data reported in the present paper. At all temperatures the values of $\mu_0 N$ extrapolated at zero density are in good agreement with those calculated using the momentum-transfer cross section of O'Malley and Crompton,[2] which is therefore very accurate also at very low energies. This gas-phase cross section is also valid at high densities, as shown by the data at high $E/N$.

These agreements are found, however, only if the neon gas used in the experiments is very accurately purified. Diatomic molecules, like $N_2$ and $O_2$, are very effective in thermalizing the drifting electrons, and therefore the results can be affected by the presence of these impurities.

The semiquantitative approach of SJC (Ref. 24) shows that, owing to multiple electron-atom interactions, the electron has not only a mean potential energy but a zero point kinetic energy as well. Retaining this qualitative idea, and taking into account the suggestion coming out from the attachment experiments, we introduced the assumption that the gas-phase scattering cross section $\sigma_M$ is to be calculated at an energy $\varepsilon^* = \varepsilon + \varepsilon_0(N)$, where $\varepsilon$ is the thermal contribution to the kinetic energy. Using the same function $\varepsilon_0(N)$ for all temperatures, it is possible to fit all the data without the introduction of adjustable parameters.

The good result obtained using a kind of self-consistent WS calculation is probably fortuitous, in the sense that it represents an approximation to the exact result to be obtained with a more rigorous treatment.

On the other hand, the idea of a dependence of $\sigma_M$ on the zero-point kinetic energy is to be regarded as more general, and it explains qualitatively the increase of $\mu_0 N$ with $N$ in gases like argon, krypton, and xenon, where $\sigma_M(\varepsilon)$ decreases rapidly with the energy toward the Ramsauer minimum.

To conclude, despite the good result of the fit based on a simple and rather general idea, there are still many problems to be solved. We believe that more experimental and theoretical work is needed for a satisfactory understanding.

## ACKNOWLEDGMENTS

We wish to acknowledge useful discussions with Professor V. Celli, Professor V. Dallacasa, and Professor G. L. Braglia. This work was supported by Consiglio Nazionale delle Richerche and Ministero Pubblica Istruzione, Rome, Italy.

[1] L. G. H. Huxley and R. W. Crompton, *The Diffusion and Drift of Electrons in Gases* (Wiley, New York, 1974).
[2] T. F. O'Malley and R. W. Crompton, J. Phys. B **13**, 3451 (1980); T. F. O'Malley *et al.*, *ibid.* **12**, 953 (1979).
[3] For a recent review, see S. R. Hunter *et al.*, in *Electron-Molecule Interactions and Their Applications*, edited by L.G. Christophorou (Academic, Orlando, 1984), Vol. II, Chap. 3.
[4] T. F. O'Malley, J. Phys. B **13**, 1491 (1980).
[5] G. L. Braglia and V. Dallacasa, Phys. Rev. A **26**, 902 (1982).
[6] W. M. Atrazhev and I. T. Iakubov, J. Phys. D **10**, 2155 (1977).
[7] K. W. Schwarz, Phys. Rev. B **21**, 5125 (1980).
[8] L. Bruschi, M. Santini, and G. Torzo, J. Phys. E **18**, 5239 (1985).
[9] L. Bruschi, M. Santini, and G. Torzo, Phys. Lett. **102A**, 102 (1984).
[10] A. Borghesani, L. Bruschi, M. Santini, and G. Torzo, Phys. Lett. **108A**, 255 (1985).
[11] L. Bruschi, R. Storti, and G. Torzo, Rev. Sci. Instrum. **56**, 427 (1985).
[12] L. Bruschi, R. Storti, and G. Torzo, Rev. Sci. Instrum. **57**, 2361 (1986).
[13] R. D. McCarty and R. B. Stewart, National Bureau of Standards No. 8726, 1965 (unpublished).
[14] We used Neon Research Grade Purity supplied by Matheson.
[15] L. Bruschi, M. Santini, and G. Torzo, J. Phys. B **1**, 1137 (1984).
[16] Oxisorb, Meissner Griesheim, Düsseldorf, West Germany.
[17] A. K. Bartels, Ph.D. thesis, University of Hamburg, 1971.
[18] A. F. Borghesani, L. Bruschi, M. Santini, and G. Torzo, Rev. Sci. Instrum. **57**, 2234 (1986).
[19] A. F. Borghesani, L. Bruschi, M. Santini, and G. Torzo, Z. Naturforsch. **41a**, 912 (1986).
[20] J. Lekner, Phys. Rev. **158**, 130 (1967).
[21] M. H. Cohen and J. Leckner, Phys. Rev. **158**, 305 (1967); S. Basak and M. H. Cohen, Phys. Rev. B **20**, 3404 (1979).
[22] B. Raz and J. J. Jortner, Chem. Phys. Lett. **9**, 222 (1971).
[23] E. Fermi, Il Nuovo Cimento **11**, 157 (1934); H. Massey and E. Burhop, *Electronic and Ionic Impact Phenomena* (Clarendon Press, Oxford, 1952), p. 178.
[24] B. E. Springett, J. Jortner, and M. H. Cohen, J. Chem. Phys. **48**, 2720 (1968).
[25] J. Bardeen, J. Chem. Phys. **6**, 367 (1938).
[26] T. P. Eggarter and M. H. Cohen, Phys. Rev. Lett. **27**, 629 (1971).
[27] L. G. Christophorou *et al.*, in *Electron-Molecule Interaction and Their Applications*, edited by L. G. Christophorou (Academic, Orlando, 1984), Vol. I, Chap. 6.
[28] A. K. Bartels, Phys. Lett. **45A**, 491 (1973).
[29] J. R. Broomall, W. D. Johnson, and D. G. Onn, Phys. Rev. B **14**, 2819 (1976).